frontiers | Frontiers in Environmental Science

TYPE Original Research
PUBLISHED 21 September 2022
DOI 10.3389/fenvs.2022.955519

Check for updates

OPEN ACCESS

EDITED BY
Guo Wen Peng,
University of South China, China

REVIEWED BY
Arpita Roy,
Sharda University, India
Rasha Sabeeh,
Al-Nahrain University, Iraq
Limin Zhou,
East China University of Technology, China

*CORRESPONDENCE
Tao Yu,
xiaoshan770@163.com

SPECIALTY SECTION
This article was submitted to Toxicology, Pollution and the Environment, a section of the journal Frontiers in Environmental Science

RECEIVED 28 May 2022
ACCEPTED 30 August 2022
PUBLISHED 21 September 2022

CITATION
Yu H, Yu T and Zeng K (2022), Prevention of radioactive pollution: A comparative simulation study on the reduction of several important radionuclides by pyrite and magnetite. *Front. Environ. Sci.* 10:955519. doi: 10.3389/fenvs.2022.955519

COPYRIGHT
© 2022 Yu, Yu and Zeng. This is an open-access article distributed under the terms of the Creative Commons Attribution License (CC BY). The use, distribution or reproduction in other forums is permitted, provided the original author(s) and the copyright owner(s) are credited and that the original publication in this journal is cited, in accordance with accepted academic practice. No use, distribution or reproduction is permitted which does not comply with these terms.

Prevention of radioactive pollution: A comparative simulation study on the reduction of several important radionuclides by pyrite and magnetite

Haoqi Yu[1], Tao Yu[1,2]* and Kai Zeng[3]

[1]Jiangxi Province Key Laboratory of Polymer Micro/Nano Manufacturing and Devices (East China University of Technology), Nanchang, China, [2]School of Nuclear Science and Engineering, East China University of Technology, East China University of Technology, Nanchang, China, [3]State Key Laboratory of Radiation Medicine and Protection, Soochow University, Suzhou, China

In order to ensure the long-term effective isolation of radionuclides from human beings to the environment, pyrite and magnetite, which exist widely and stably in the geological environment, can be considered to reduce the strong mobility of high-valence redox-sensitive nuclides to the low-valence nuclides with low mobility. In this work, the reducing reaction between pyrite, magnetite, and redox-sensitive radionuclides (U, Se, Tc, and Np) in the Gansu proposed-treatment plant area was under simulation by PHREEQC. Due to the considerable existence of quartz and calcite in the Gansu proposed-treatment plant area surrounding the rock of interest, the influence of the dissolved Ca^{2+} and SiO_3^{2-} should be taken into account. The corresponding precipitation saturation index of the complex (UO_X, Se(s), and TcO2) and species of interest was calculated, and the results suggested that pyrite can significantly reduce the high-valence radionuclides (U, Se, Tc, and Np), and their corresponding precipitation saturation indexes (SIs) were usually positive. However, magnetite, in a given condition, showed a certain reducing effect against Se and Np and a poor effect on U and Tc. It was worth noting that the aqueous pH in the system always remained constant because of the CO_2 partial pressure of the underground biosphere under this long-term time scale. These conclusions have an important guiding significance for the prevention and retention of radioactive pollution released into the biological environment.

KEYWORDS

pyrite, magnetite, saturation index, simulation, radionuclides

1 Introduction

Nuclear energy, due to its advantages of durability, economy, security, and cleanliness, has been considered one of the most developed potential and valuable energy. However, with the rapid development of nuclear energy, radioactive wastes have been inevitably generated and accumulated during the operation and decommissioning of nuclear power plants. If not properly resolved, it will seriously hinder the sustainable development of nuclear energy (Wu et al., 2013). Currently, according to the radioactive degree of radioactive wastes, they could be divided into low-, medium-, and high-level radioactive wastes. Meanwhile, high-level radioactive wastes are usually disposed of in a way of deep geological disposal (Grambow, 2008). After long-term storage, the disposal facility will eventually be damaged, which will further cause the migration of the radionuclides by groundwater into the surrounding rock medium (Wang et al., 2005; Vanloon et al., 2012). However, for the long-term effective isolation of radioactive wastes, pyrite and magnetite, existing widely and stably in the geological environment, have been considered to reduce the strong mobility of high-valence redox-sensitive radionuclides (U, Se, Tc, and Np) to a low-valence state with a weak mobility state to make these low-valence radionuclides adhere to the surrounding rock medium (Bruggeman et al., 2002; Bruggeman et al., 2005; Eglizaud et al., 2006; Naveau et al., 2007). At present, numerous previous studies (Kang et al., 2014; Ma et al., 2014; Ma et al., 2020; Hu et al., 2022a; Hu et al., 2022b; Luo et al., 2022) have been carried out on the reduction experiments of U(VI) and Se(VI) by pyrite and magnetite, and the results indicated that a high-valence state of U(VI) and Se(VI) can be successfully reduced to U(IV) and Se(0) in a low-valence state, respectively, which is easily adsorbed and migrated with difficulty. Moreover, bacteria have been widely used to reduce high-valence redox-sensitive radionuclides for bioremediation (He et al., 2021; You et al., 2021). Meanwhile, natural minerals were also widely used to investigate the adsorption of key radionuclides to prevent them from being released into the biosphere (Yu et al., 2020). However, owing to the limitations such as the time scale of the actual physical experiments and the inability to quantify the number of reactants used, it is a choice of major importance to calculate the reaction under a specific system by geochemical simulation software through the relevant thermodynamic database (Metz et al., 2003; Vitorge and Capdevila, 2003; Windt et al., 2006). For instance, the reduction of U(VI), Se(VI), and Tc(VII) was under simulation in the Beishan underground water environment by the geochemical software PHREEQC (Version 2.15.02), and its calculated results showed that the concentrations of U(VI), Se(VI), and Tc(VII) could be effectively reduced by pyrite (Kang et al., 2010). Furthermore, unstable silicate and carbonate minerals in the surrounding rock medium of the Beishan underground areas will affect the concentrations of calcium ion, silicate, and carbonate in this simulated underground environment, which will further influence the species of U, Se, and Tc. Therefore, it is necessary to consider the influence of silicate and carbonate minerals.

TABLE 1 Chemical composition of the groundwater taken from the Gansu proposed-treatment plant area.

Ion	C/(mg·L^{-1})	Ion	C/(mg·L^{-1})
Na^+	365	F^-	0.87
Ca^{2+}	89.6	Cl^-	578
Mg^{2+}	45.4	NO_3^-	<0.08
K^+	19	SO_4^{2-}	78.4
pH	~7.95		

In order to accurately describe the geochemical reactions while the radionuclides migrate from the artificial barrier into the natural barrier by groundwater between the liquid and mineral phase including adsorption, migration, and diffusion behavior, numerous relevant types of geochemical software have been developed to simulate the relevant complex reaction procedure. At present, there are various types of representative geochemical software, such as PHREEQCI (USGS, 2017; Parkhurst and Appelo, 1999), WATEQ4F (Ball and Nordstrom, 1991), MINEQL (Westall, 1976), FITEQL (Heberlin and Westall, 1996), MINTEQA2 (Allison et al., 1991), and EQ3/6 (Wolery and Jarek, 2003). In this work, the reduction of several important radionuclides (U(VI), Se(VI), Tc(VII), and Np(V)) by pyrite and magnetite in the Gansu proposed-treatment plant area's conditions was under simulation by PHREEQC using the THERMOCHIMIE-TDB 10a database from ANDRA/RWM of France. Also, these results will give an important reference for the related field experiments.

2 Theory and simulation conditions

2.1 Definition of the saturation index

The procedure of precipitation/dissolution of minerals in the groundwater is determined by the saturation index (SI) value, which is mathematically expressed as follows:

$$\mathbf{SI} = \mathbf{lg}\left(\frac{\mathbf{IAP}}{\mathbf{K}}\right). \quad (1)$$

Here, IAP is the ionic activity product and K is the solubility product constant of the mineral. Theoretically, SI = 0 means that the precipitation or dissolution reactions of minerals are in equilibria with the groundwater; SI > 0 indicates that the

TABLE 2 Various key numerical values used (model input) in PHREEQC.

#Condition	Input value	Reference
Set concentration of radionuclides of interest (U, Se, Tc, and Np)	1.0×10^{-4} mol L^{-1}	Kang et al. (2010)
Chemical composition of an aqueous reaction	Listed in Table 1	Xie et al. (2021)
Set SI of calcite	SI = 0.5	Dou et al. (2010)
Set SI of quartz	SI = 0.2	Guo et al. (2016)
CO_2 partial pressure	10^{-3} bar	In this work (for controlling the pH)

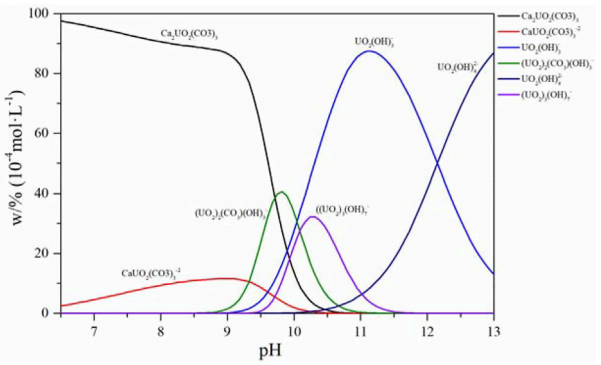

FIGURE 1
Effect of pH on the species of U in groundwater.

minerals are supersaturated and the minerals tend to produce precipitation; SI < 0 means that the mineral is unsaturated and the minerals tend to dissolve.

In PHREEQC software, the redox potential is expressed in terms of the electron potential pe value, and its quantitative relationship with the redox potential (Eh) can be expressed by Eq. 2:

$$\mathbf{pe} = \left(\mathbf{F}^{*}\frac{\mathbf{Eh}}{\mathbf{2.303RT}}\right), \tag{2}$$

where F is the Faraday constant (96,484 C/mol), R is the molar gas constant (8.314j/(Kmol)), and T is the Kelvin temperature K.

2.2 Simulation conditions

In this work, in a system of the field groundwater of the proposed disposal plant environment, the reduction reactions of radionuclides (U, Tc, Se, and Np) by magnetite and pyrite were conducted. The chemical composition of the groundwater is shown in Table 1 (Xie et al., 2021). The ionic strength of this groundwater was calculated to be about 0.026 mol/L, which is consistent with the applicability of the Davis equation and the WATEQ Debye–Hückel equation in PHREEQC.

In order to simulate whether the reduction effect by pyrite and magnetite was significant for radionuclides at a relatively higher concentration, the initial concentration of radionuclides in this simulation was set to 1.0×10^{-4} mol L^{-1}. If the subsurface environmental system was completely considered as a closed system, only the solid–liquid phase equilibrium needed to be considered, and the partial pressures of oxygen and carbon dioxide in the actual atmospheric pressure did not need to be considered. However, pH calculated in this groundwater (pH = 9.21) deviated from the actual measured value (pH = 7.95), and the gas phase equilibrium needed to be considered to control the pH of the solution. However, if the partial pressure of oxygen in the atmosphere was considered, the redox potential in this simulated system will always be oxidizing caused by the continuous dissolved oxygen. Generally, the partial pressure of atmospheric CO_2 is about $10^{-3.5}$ bar, while in the biologically active geosphere, it will be higher than in the atmosphere (Merkel and Paner-Friedrich, 2005). Based on the deviation between the actual measured pH (7.95) and the simulated pH (9.21), the effect of atmospheric CO_2 partial pressure needed to be taken into account, thus inferring the CO_2 partial pressure in a gas-phase equilibrium was calculated to be $10^{-3.0}$ bar. Moreover, the composition of the surrounding rock will also affect the migration of radionuclides in the fractures or cracks of the surrounding rock. The proposed treatment plant area in Gansu is enriched with clay minerals including granite and calcite (Xie et al., 2021). Therefore, the influence of the dissolution of quartz and calcite in this reaction process should be considered. Theoretically, SI = 0 indicates that the minerals reach an equilibrium state with the groundwater, but in practice, nucleation of secondary minerals is more difficult at room temperature and requires a supersaturating driving force. Therefore, precipitation will only occur where the saturation index (SI) is greater than zero. The results of the previous study (Dou et al., 2010) show that the saturation index of calcite precipitation in granitic areas is about 0.5. In Table 1, the silicon concentration is not observed. By virtue of the estimated saturation index of silica-bearing secondary minerals illite, kaolinite, calcium, and sodium-based montmorillonite precipitation in granitic areas and subsequently the inversed saturation index of quartz

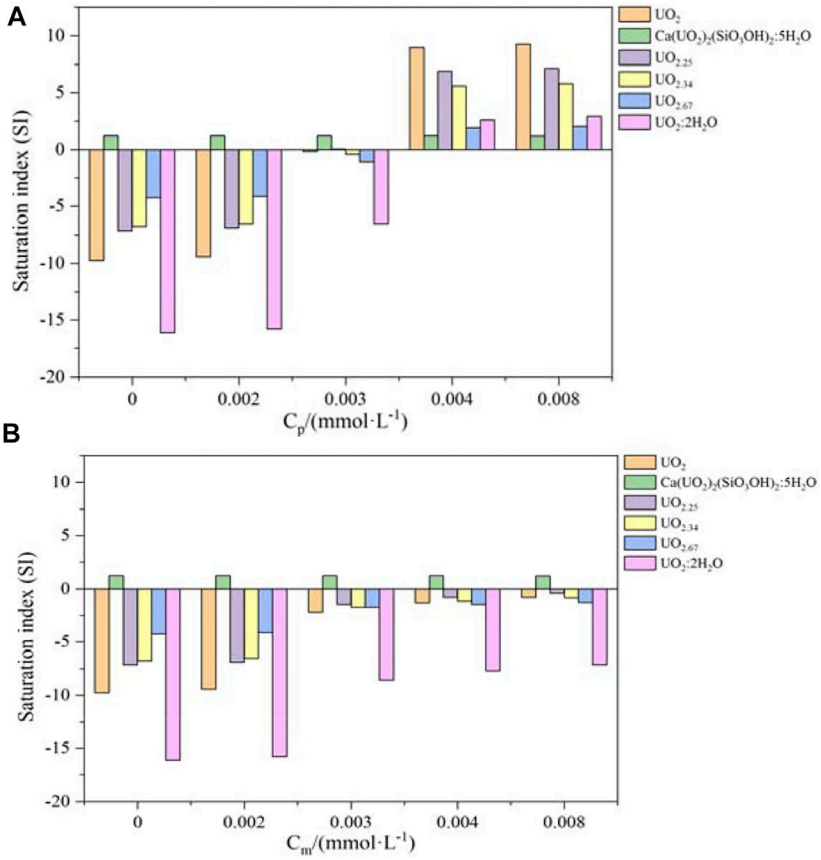

FIGURE 2
Saturation index evolution of the precipitation of U(IV) as a function of pyrite **(A)** and magnetite **(B)**.

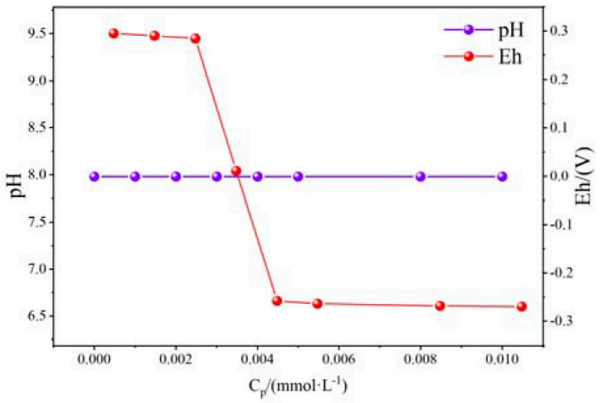

FIGURE 3
pH and Eh as functions of the pyrite concentration.

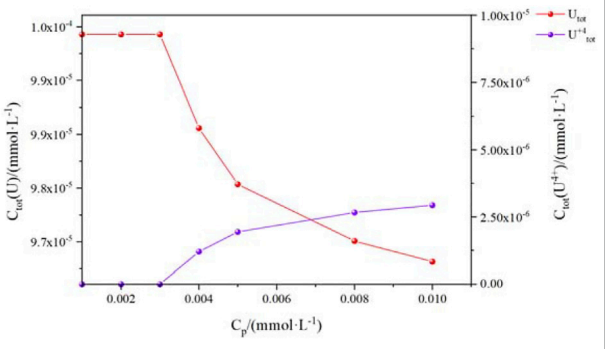

FIGURE 4
Concentration of U_{tot} and U $(+4)_{tot}$ as functions of pyrite concentration.

through the liquid–solid equilibrium by PHREEQC (Guo et al., 2016), the saturation index of quartz was estimated to be 0.2, thereby controlling the silicon dissolution of the groundwater environment. Conveniently, the various key numerical values used (model input) and their corresponding references are listed in Table 2.

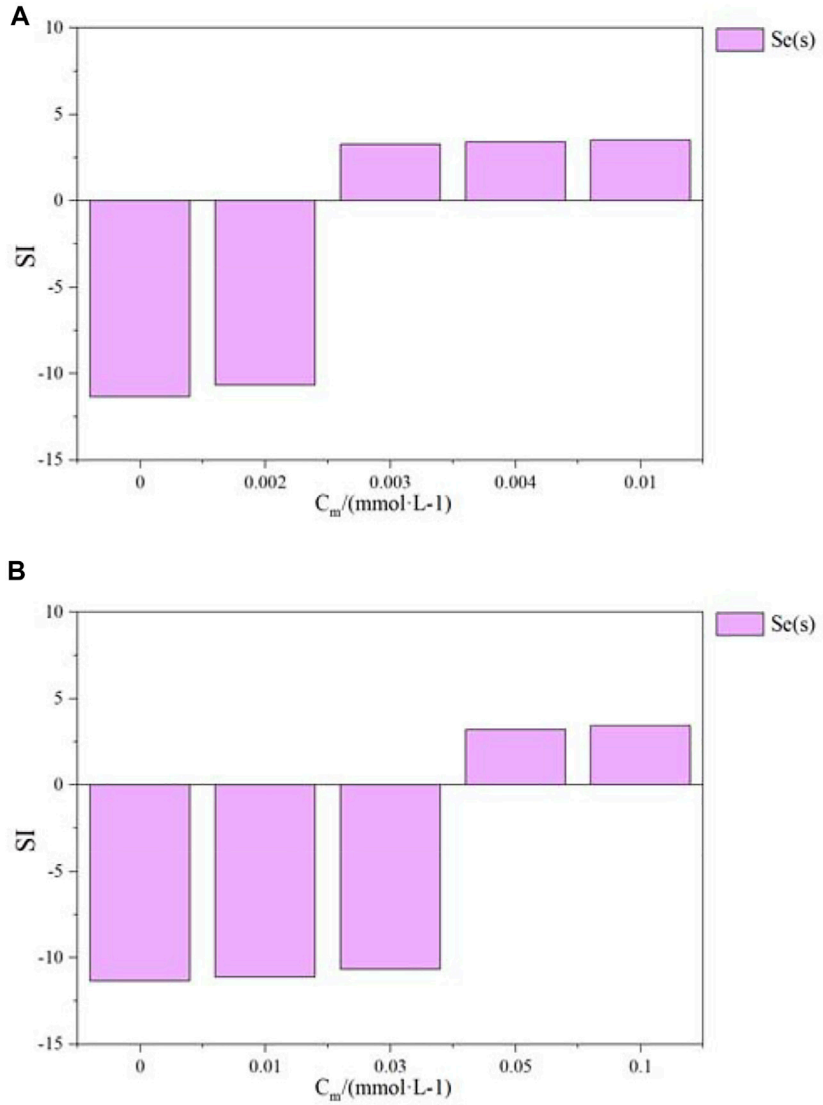

FIGURE 5
Saturation index evolution of the precipitation of Se(s) as a function of pyrite **(A)** and magnetite **(B)**.

3 Results and discussion

3.1 Reduction of U by magnetite and pyrite

In the process of disposal of high-level wastes, uranium, as the main component of spent fuel, will seriously damage the ecological environment and human beings once it migrates to the biosphere with groundwater. The migration properties of uranium are strongly determined by its oxidation form, and U(VI) has strong migration properties in the geological environment, while U(IV) with poor solubility is easily precipitated. The effect of pH on species of U in groundwater was plotted by PhreePlot software (later handwork by origin software) and is shown in Figure 1.

Unstable calcite minerals also supplied a source of Ca (Cai et al., 2007). As shown in Figure 1, uranium dominated as $Ca_2UO_2(CO_3)_3$ (aq) in an aqueous solution at the pH range of 7–9. Also, with the increase in pH, the uranyl complexations existed in the form of $(UO_2)_2(CO_3)(OH)_3^-$, $(UO_2)_3(OH)_7^-$, $UO_2(OH)_3^-$, and $UO_2(OH)_4^{2-}$. Moreover, the actual measured value of pH in this proposed treatment plant's groundwater was 7.95, indicating that U(VI) was the species of $Ca_2UO_2(CO_3)_3$ (aq) in this environment, and it mainly accounted for

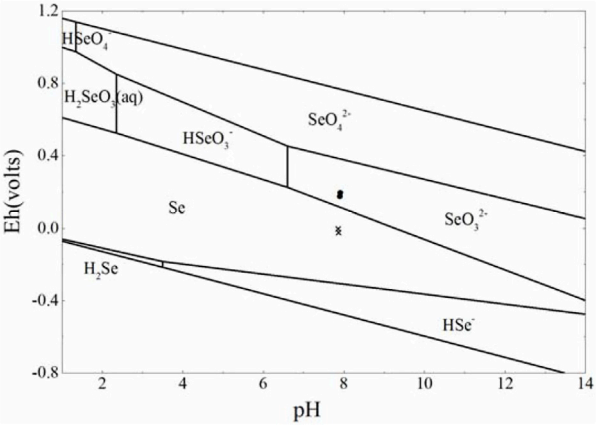

FIGURE 6
Pourbaix diagrams produced by PhreePlot (Parkhurst and Appelo, 1999; PhreePlot Guide, 2020) using the THERMOCHIMIE-TDB 10a database from ANDRA/RWM of France (re-plotted by handwork). The following conditions have been used for groundwater and $[Se]_{tot} = 10^{-4}$ mol L^{-1}. The upper and lower boundaries are the stable boundaries of H_2O.

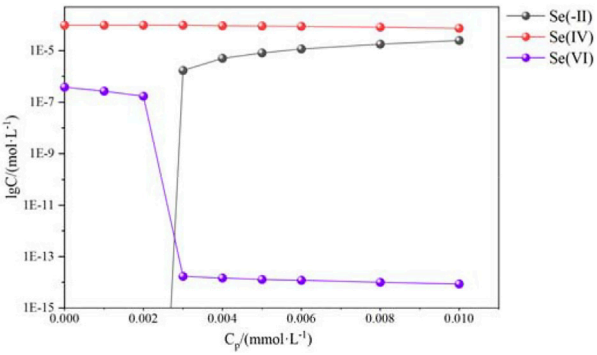

FIGURE 7
Log C of Se(-II), Se(IV), and Se(IV) as a function of the pyrite concentration.

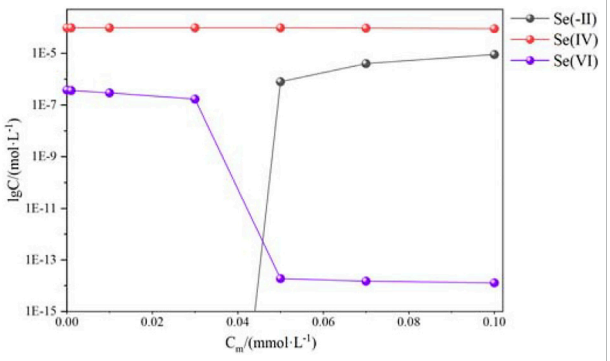

FIGURE 8
Log C of Se(-II), Se(IV), and Se(IV) as a function of the magnetite concentration.

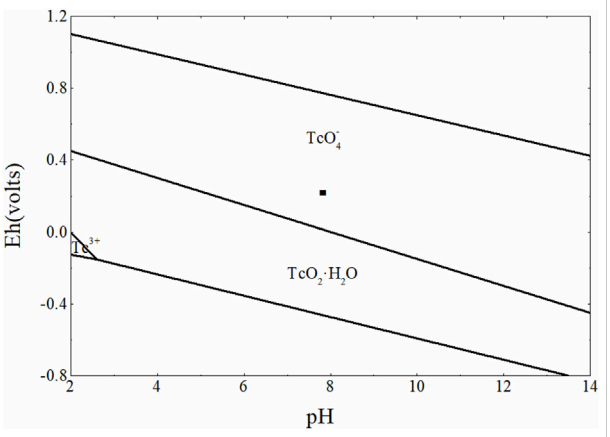

FIGURE 9
Eh-pH diagram of [Tc]tot = 10^{-4} mol L^{-1} under the groundwater taken from the Gansu proposed-treatment plant area.

88.52% of the total amount of U (VI) (8.85×10^{-5} mol L^{-1}). This was slightly different from the results of the previous study (Merkel and Paner-Friedrich, 2005), which suggested that uranyl carbonate absolutely dominated this groundwater environment. It is because the dissolution of calcite and quartz in the surrounding rock would increase the concentration of Ca^{2+} and SiO_3^{2-}, which further take the complexation reactions between the uranyl carbonate and calcium or silicate ions. Also, these calculation results were consistent with the Eh-pH diagram for uranium in the groundwater of Beishan that contained unstable calcite in the previous study (Qin and Kang, 2017).

A comparative analysis of the uranium reduction reactions by pyrite and magnetite has been performed. Subsequently, the saturation index of different complex oxides of U (IV) as a function of pyrite and magnetite is shown in Figure 2. With the concentration of pyrite and magnetite being increased, the SI of the complex oxide of U(IV) shown in Figure 2A all increased in different magnitudes. When the amount of pyrite used (C_p) increased from 0.003 mmol L^{-1} to 0.004 mmol L^{-1}, the SI of UO_2 increased from F02D 0.16 to 8.94, and the SI of $UO_{2.25}$, $UO_{2.34}$, $UO_{2.67}$, and $UO_2.2H_2O$ all also increased in a relatively large magnitude. It was worth noting that the SI of $Ca(UO_2)_2(SiO_3OH)_2.5H_2O$ was always greater than zero in this groundwater environment. Once the amount of pyrite

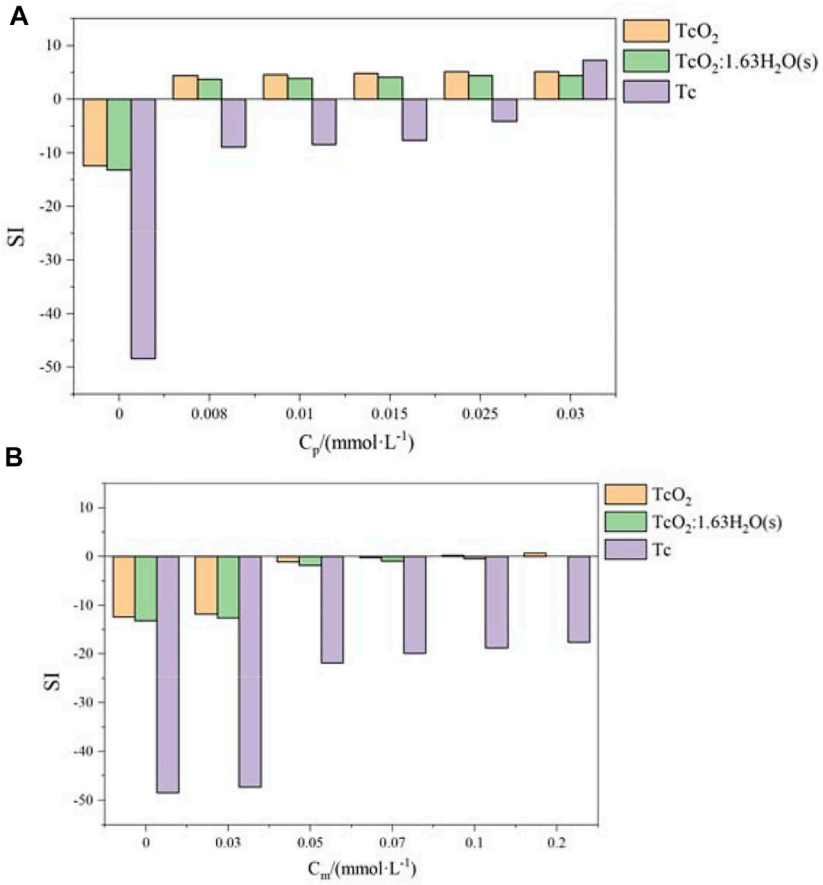

FIGURE 10
Saturation index evolution of the precipitation of TcO2(cr), Tc, and TcO2.1.63H2O(s) as a function of pyrite **(A)** and magnetite **(B)**.

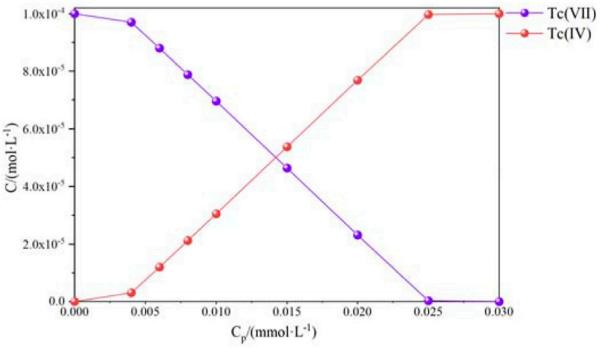

FIGURE 11
Concentration of Tc(VII) and Tc(IV) as a function of the pyrite concentration.

used reached 0.004 mmol L^{-1}, all the complex oxides of U(IV) shown in Figure 2A tended to precipitate. According to Figure 2B, the SI of the complex oxide of U(IV) was less than zero, except for $Ca(UO2)_2(SiO_3OH)_2.5H_2O$ (SI > 0), indicating that under the same conditions, magnetite was poor in reducing U(VI) in this environment compared to pyrite. This was also consistent with the results of the previous study (Ma et al., 2020; Luo et al., 2022) on the reduction of U(VI) by magnetite, and only at an acidic condition, U(VI) can be successfully reduced. When considering the dissolution of calcite and quartz, the concentration of calcium and silicate ions increased from 2.236×10^{-3} mol L^{-1} to 3.124×10^{-3} mol/L and from zero to1.843×10^{-6} mol L^{-1}, respectively. This would further conduct the complexation reactions with UO_2^{2+} to produce the insoluble oxide of $Ca(UO_2)_2(SiO_3OH)_2.5H_2O$. Therefore, the groundwater environment in this area was favorable to slow down the migration behavior of U(VI).

As shown in Figure 3, the pH value remained constant, while the Eh value changed significantly with the amount of pyrite used, and the Eh value dropped to -258 mV at Cp = 0.004 mmol-L^{-1}. This was different from the results of the

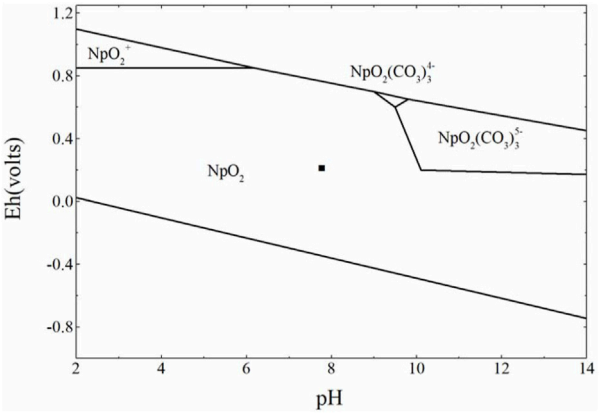

FIGURE 12
Eh-pH diagram of [Np]tot = 10^{-4} mol L^{-1} under the groundwater taken from the Gansu proposed-treatment plant area.

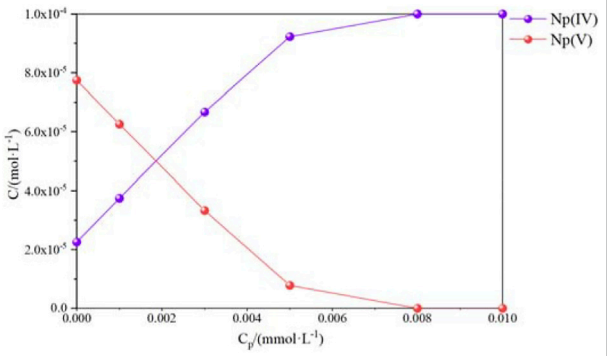

FIGURE 13
Concentration of Np(IV)and Np(V) as a function of the pyrite concentration.

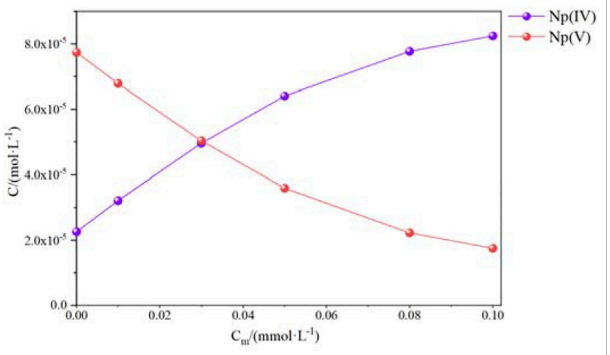

FIGURE 14
Concentration of Np(IV)and Np(V) as a function of the magnetite concentration.

change in pH with the increase of pyrite or magnetite used in the previous work (Liger et al., 1999; Yan et al., 2022). The main reasons for this difference could be 1) the partial pressure of atmospheric carbon dioxide considered in this work consistently controlled the pH of the solution; therefore, the pH of this system remained constant; and 2) the amount of pyrite used in this work was too small to cause significant pH changes.

The change in the total U(VI) and $U(+4)_{tot}$ concentrations is shown in Figure 4. With the increase in pyrite used, the total concentration of U(VI) gradually decreased, yet the concentration of $U(+4)_{tot}$ increased. When the amount of pyrite used was 0.004 mmol L^{-1}, the Eh value presented a strongly reduced state. At the same time, the concentration of U_{tot} appeared to show a sudden drop point, from 1.0×10^{-4} mol-L^{-1} decreasing to 0.988×10^{-4} mol L^{-1}, while the concentration of $U(+4)_{tot}$ increased from 0 to 1.21×10^{-6} mol L^{-1}

3.2 Reduction of Se by magnetite and pyrite

^{79}Se (with a half-life of 2.95×10^5 years) has been considered to be one of the key migrating fission products that are generated during the disposal of spent fuel and high-level radioactive wastes (Jiang et al., 2001; Charlet et al., 2012).[79] Se is a variable-valence nuclide sensitive to redox conditions, and its valence states are present including Se(-II), Se(-I), Se, Se(IV), and Se(VI) in the natural environment. Its solubility and mobility are strongly determined by the valence state (Chen et al., 1999), and Se(IV) is not only highly soluble in the aqueous solution but is also difficult to be adsorbed by backfill engineering and surrounding rock materials located at the near-field geochemical environment of the repository.

As shown in Figure 5, both pyrite and magnetite can reduce Se(IV) to Se(s) precipitates. Previous studies (Breynaert et al., 2008; Kang et al., 2014) experimentally demonstrated that pyrite can reduce Se(IV) to Se(0). The redox transformations of Se(IV) in the presence of Fe-bearing minerals have been successfully demonstrated, and the specific mechanism of electron transfer reactions was also investigated (Kim et al., 2017). The present work further confirmed that the same effect can be achieved with magnetite, but the reduction performance of magnetite was not as strong as pyrite.

As shown in Figure 6, SeIV mainly existed in the species of selenate hydrogen (SeO_3^{2-}) in this groundwater environment, and the black circle/fork symbols represented the before and

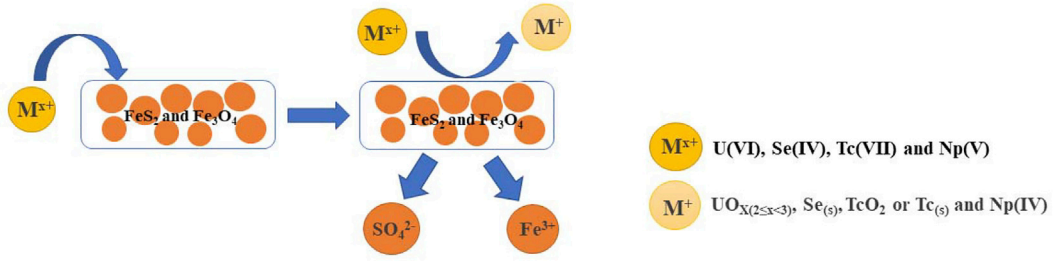

FIGURE 15
Scheme of mechanism for reduction behavior.

after reactions. It indicated that $SeO_3^{2-}$was thermodynamically reduced to Se(s) during the whole reaction process. In order to further investigate the change of different valence states of Se concentration as the amount of pyrite and magnetite used increased, the following simulations were carried out and the results are shown in Figure 7.

As shown in Figure 7, Se mainly existed in the species of Se(IV), and its concentration was 9.96×10^{-5} mol L^{-1}, with a small amount of Se (VI) presented simultaneously at a concentration of 3.8×10^{-7} mol L^{-1}. When the amount of pyrite used was more than 0.003 mmol L^{-1}, the Se(IV) concentration was continuously decreased from 9.98×10^{-5} mol L^{-1} to 9.83×10^{-5} mol L^{-1} and Se (-II) was significantly continuously increased. The previous study (Kang et al., 2013) demonstrated the reduction mechanism of Se by pyrite, and these results suggested that the function of Fe(II) of pyrite was to act as an electron conductor, and eventually, S_2^{2-} was oxidized.

As shown in Figure 8, Se(IV) could also be effectively reduced by magnetite, yet the amount of magnetite used was considerably greater than pyrite used in these specific conditions. The aforementioned results suggested that both pyrite and magnetite could reduce Se(IV); however, the magnetite reduction capacity is much lower than that of pyrite.

3.3 Reduction of Tc by magnetite and pyrite

^{99}Tc with a half-life of 2.13×10^5 years exists at +4, 6, and 7 valences and is mainly presented in a stable state for pertechnetate (TcO_4^-) with strong mobility and solubility. Previous studies (Cui and Eriksen, 1996; Dejun et al., 2004) showed experimentally that the adsorption mechanisms of^{99} Tc in Fe, Fe_2O_3, and Fe_3O_4 were different, and pyrite could effectively reduce Tc(VII) to the low solubility oxide of Tc (IV) (Huo et al., 2017; Rodriguez et al., 2021).

As shown in Figure 9, Tc mainly existed as TcO_4^- in the groundwater solution environment of a proposed treatment plant in Gansu. With the redox potential decreased, TcO_4^- was reduced to the insoluble oxide of $TcO_2{\cdot}H_2O$ with crystalline water. This suggested that this environment system was not conducive to the geological disposal of Tc. The precipitation saturation index (SI) of the related insoluble oxide of Tc(IV) and Tc(0) with the different amounts of pyrite and magnetite used is shown in Figure 10.

The SI of insoluble oxides and monomers of Tc was less than 0 in the initial solution, as shown in Figure 10B. When the magnetite used (C_m) increased above 0.1 mmol L^{-1}, the SI of TcO_2 and $TcO_2.1.63H_2O$ was close to 0 (SI~0) and the SI of Tc (0) was much less than 0. However, the SI of secondary minerals in groundwater to be slightly greater than 0 was common, and mineral precipitation requires nucleation-free energy to overcome nucleation resistance (Breynaert et al., 2008). Therefore, the reduction of Tc(VII) by magnetite would not necessarily lead to precipitation. Moreover, according to Figure 10A, the SI of TcO_2 and $TcO_2.1.63H_2O$ was much greater than 0, once the amount of pyrite used reached 0.008 mmol L^{-1}. These results indicate that compared to magnetite, pyrite exhibited a stronger reduction performance. As shown in Figure 11, Tc(VII) was effectively reduced with the increase of pyrite used. When the amount of pyrite used reached 0.03 mmol L^{-1}, all of Tc(VII) were totally reduced to Tc(IV).

3.4 Reduction of Np by magnetite and pyrite

Although the initial concentration of ^{237}Np (with a half-life of 2.14×10^6 years) as a long-lived radionuclide is relatively low in spent fuel, the decay product of ^{241}Pu and ^{241} Am,^{237} Np,

also becomes a major contributor to radiotoxicity after a long period of deep geological disposal (Kaszuba and Runde, 1999). The oxidation states of Np exist from III to VII valence; however, for geological disposal, the most important valence of Np is Np(IV) and Np(V), and compared to Np(IV), Np(V) has a stronger migration property and needs more close attention.

According to the Eh-pH diagram in Figure 12, the speciation of Np was primary NpO_2 in this simulated environment and a small amount of $NpO_2.2H_2O$ and Np_2O_5 oxide precipitates was also presented. This observed phenomenon showed that this groundwater environment was beneficial to slow down the migration of Np.

As shown in Figure 13, the species of Np were proportionally presented in two valence forms (Np(IV) and Np(V)). The concentrations of Np(IV) and Np(V) in the initial system conditions were 2.26×10^{-5} mol L^{-1} and 7.74×10^{-5} mol L^{-1}, respectively. With the increase of the pyrite used, the Np(V) concentration decreased significantly and all the Np(V) was totally reduced to Np(IV), once the pyrite use reached 0.01 mmol L^{-1}. The concentrations of Np(IV) and Np(V) as a function of magnetite concentration are shown in Figure 14. The same consequence was demonstrated that compared to magnetite, pyrite showed a strong reductive capability according to the input amount used, and both magnetite and pyrite could successfully work.

4 Conclusion

In this work, we discuss the speciation of U, Se, Tc, and Np and their corresponding precipitation saturation indexes of the precipitates produced by pyrite and magnetite in this regional environment. Taking the groundwater of a proposed reprocessing plant in Gansu as an example and discussing the comparison of the reduction performance of the two minerals, the mechanism scheme for the reduction behavior is shown in Figure 15. The results showed that pyrite can effectively reduce the high-valence state of U, Se, Tc, and Np and easily migrate to the low-valence oxide species, which are difficult to migrate and easy to precipitate. In contrast, magnetite has a certain reduction effect on Se and Np but a poor effect on U and Tc. The simulation results not only theoretically illustrate the feasibility of the reduction of radionuclides by pyrite and magnetite but also quantify their reaction depth. However, the kinetic effects and the influence of the partial pressure of oxygen in the atmosphere on the process were not considered in this work. Hence, there will be some deviations in the actual process, and these conclusions have an important guiding significance for the prevention and retention of radioactive pollution released into the biological environment.

Data availability statement

The original contributions presented in the study are included in the article/Supplementary Material; further inquiries can be directed to the corresponding author.

Author contributions

The experiments and writing of the manuscript were mainly conducted by the first author. The supporting fund and revision were all conducted by the corresponding author.

Funding

This project was financially supported by the Natural Science Foundation of Jiangxi Province, China (20202BABL203004), the Opening Project of Jiangxi Province Key Laboratory of Polymer Micro/Nano Manufacturing and Devices (PMND202101), and the Project of State Key Laboratory of Radiation Medicine and Protection, Soochow University (No. GZK1202117).

Conflict of interest

The authors declare that the research was conducted in the absence of any commercial or financial relationships that could be construed as a potential conflict of interest.

The reviewer LZ declared a shared affiliation with the authors to the handling editor at the time of review.

Publisher's note

All claims expressed in this article are solely those of the authors and do not necessarily represent those of their affiliated organizations, or those of the publisher, the editors, and the reviewers. Any product that may be evaluated in this article, or claim that may be made by its manufacturer, is not guaranteed or endorsed by the publisher.

References

Breynaert, E., Bruggeman, C., and Maes, A. (2008). XANES-EXAFS analysis of Se solid-phase reaction products formed upon contacting Se(IV) with FeS_2 and FeS. *Environ. Sci. Technol.* 42, 3595–3601. doi:10.1021/es071370r

Bruggeman, C., Maes, A., Vancluysen, J., and Vandemussele, P. (2005). Selenite reduction in boom clay: Effect of FeS_2 clay minerals and dissolved organic matter. *Environ. Pollut.* 137, 209–221. doi:10.1016/j.envpol.2005.02.010

Bruggeman, C., Vancluysen, J., and Maes, A. (2002). New selenium solution speciation method by ion chromatography plus gamma counting and its application to FeS_2-controlled reducing conditions. *Radiochim. Acta* 90, 629–635. doi:10.1524/ract.2002.90.9-11_2002.629

Cai, C., Dong, H., Li, H., Xiao, X., Ou, G., and Zhang, C. (2007). Mineralogical and geochemical evidence for coupled bacterial uranium mineralization and hydrocarbon oxidation in the Shashagetai deposit. NW China. *Chem. Geol.* 236, 167–179. doi:10.1016/j.chemgeo.2006.09.007

Charlet, L., Kang, M., Bardelli, F., Kirsch, R., Gehin, A., Greneche, J. M., et al. (2012). Nanocomposite pyrite–greigite reactivity toward Se(IV)/Se(VI). *Environ. Sci. Technol.* 46, 4869–4876. doi:10.1021/es204181q

Chen, F., Peter, C. B., and Rodney, C. E. (1999). ^{79}Se: Geochemical and crystallo-chemical retardation mechanisms. *J. Nucl. Mater.* 275, 81–94. doi:10.1016/s0022-3115(99)00105-1

Cui, D. Q., and Eriksen, T. E. (1996). Reduction of pertechnetate by ferrous iron in solution: Influence of sorbed and precipitated Fe(II). *Environ. Sci. Technol.* 30, 2259–2262. doi:10.1021/es9506263

Dejun, L., Xianhua, F., Yingjie, Z., Jun, Y., Duo, Z., and Yong, W. (2004). Study on adsorption of ^{99}Tc on Fe, Fe_2O_3 and Fe_3O_4. *J. Nucl. Radio.* 26, 23–28.

Dou, S., Chen, F., Yang, Y., Wu, S., Kang, M., and Rong, Z. (2010). Estimation of saturation index for the precipitation of secondary minerals during water-rock interaction in granite terrains. *Geochimica* 39, 326–336.

Eglizaud, N., Miserque, F., Simoni, E., Schlegel, M., and Descostes, M. (2006). Uranium(VI) interaction with pyrite (FeS_2):chemical and spectroscopic studies. *Radiochim. Acta* 94, 651–656. doi:10.1524/ract.2006.94.9-11.651

Grambow, B. (2008). Mobile fission and activation products in nuclear waste disposal. *J. Contam. Hydrol.* 102, 180–186. doi:10.1016/j.jconhyd.2008.10.006

Guo, H., Kang, M., Chen, W., Long, J., and Zhun, Z. (2016). Speciation and solubility if americium in Beishan groundwater. *Radiat. Prot.* 36, 40–46.

He, S., Hu, W., Liu, Y., Xie, Y., Zhou, H., Wang, X., et al. (2021). Mechanism of efficient remediation of U(VI) using biogenic CMC-FeS complex produced by sulfate-reducing bacteria. *J. Hazard. Mat.* 420, 126645. doi:10.1016/j.jhazmat.2021.126645

Hu, X. W., Yang, X. Y., Wu, Z. J., Ren, Y. S., and Miao, P. S. (2022). Sedimentological, petrological, and geochemical constraints on the formation of the Beisantai sandstone-type uranium deposit, Junggar Basin, NW China. *Ore Geol. Rev.* 141, 104668. doi:10.1016/j.oregeorev.2021.104668

Hu, X. W., Yang, X. Y., Ren, Y. S., Du, G. F., and Wu, Z. J. (2022). Genesis of interlayer oxidation zone-type uranium deposit in the channel conglomerates, Beisantai area, Junggar Basin: An insight into uranium mineralization. *Ore Geol. Rev.* 140, 104557. doi:10.1016/j.oregeorev.2021.104557

Huo, L., Xie, W., Qian, T., Guan, X., and Zhao, D. (2017). Reductive immobilization of pertechnetate in soil and groundwater using synthetic pyrite nanoparticles. *Chemosphere* 174, 456–465. doi:10.1016/j.chemosphere.2017.02.018

Jiang, S., He, M., Diao, L., Guo, J., and Wu, S. (2001). Remeasurement of the half-life of ^{79}Se with the projectile X-Ray detection method. *Chin. Phys. Lett.* 18, 746–749. doi:10.1088/0256-307x/18/6/311

Kang, M., Chen, F., Yang, Y., Wu, S., and Dou, S. (2010). Modelling the reactive-path between pyrite and radioactive nuclides. *J. Nucl. Radio.* 32, 160–166.

Kang, M. L., Fabrizio, B., Laurent, C., Antoine, G., Andrey, S., Cheng, F. R., et al. (2014). Redox reaction of aqueous selenite with As-rich pyrite from Jiguanshan ore mine (China): Reaction products and pathway. *Appl. Geochem.* 47, 130–140. doi:10.1016/j.apgeochem.2014.05.018

Kang, M., Ma, B., Fabrizio, B., Chen, F., Liu, C., Zheng, Z., et al. (2013). Interaction of aqueous Se(IV)/Se(VI) with FeSe/$FeSe_2$: Implication to Se redox process. *J. Hazard. Mat.* 248-249, 20–28. doi:10.1016/j.jhazmat.2012.12.037

Kaszuba, J. P., and Runde, W. H. (1999). The aqueous geochemistry of neptunium: Dynamic control of soluble concentrations with applications to nuclear waste disposal. *Environ. Sci. Technol.* 33, 4427–4433. doi:10.1021/es990470x

Kim, Y., Yuan, K., Ellis, B. R., and Becker, U. (2017). Redox reactions of selenium as catalyzed by magnetite: Lessons learned from using electrochemistry and spectroscopic methods. *Geochimica Cosmochimica Acta* 199, 304–323. doi:10.1016/j.gca.2016.10.039

Liger, E., Charlet, L., and Cappellen, P. V. (1999). Surface catalysis of uranium(VI) reduction by iron(II). *Geochimica Cosmochimica Acta* 63, 2939–2955. doi:10.1016/s0016-7037(99)00265-3

Luo, G., Zhang, T., Yuan, Z., Fu, Z., Lv, S., Huang, C., et al. (2022). Removal of hexavalent uranium [U(VI)] by magnetite in the presence of metal-reducing bacteria from rice soil. *Environ. Technol. Innov.* 28, 102616. doi:10.1016/j.eti.2022.102616

Ma, B., Kang, M., Zheng, Z., Cheng, F., Xie, J., Laurent, C., et al. (2014). The reductive immobilization of aqueous Se(IV) by natural pyrrhotite. *J. Hazard. Mat.* 276, 422–432. doi:10.1016/j.jhazmat.2014.05.066

Ma, Y., Cheng, X., Kang, M., Yang, G., Yin, M., Wang, J., et al. (2020). Factors influencing the reduction of U(VI) by magnetite. *Chemosphere* 254, 126855. doi:10.1016/j.chemosphere.2020.126855

Merkel, B. J., and Paner-Friedrich, B. (2005). *The principle and application of groundwater geochemical modeling*. Wu Han: China University of Geoscience.

Metz, V., Kienzler, B., and Schussler, W. (2003). Geochemical evaluation of different groundwater-host rock systems for radioactive waste disposal. *J. Contam. Hydrol.* 61, 265–279. doi:10.1016/s0169-7722(02)00130-4

Naveau, A., Monteil-Rivera, F., Guillon, E., and Dumonceau, J. (2007). Interactions of aqueous selenium (–II) and (IV) with metallic sulfide surfaces. *Environ. Sci. Technol.* 41, 5376–5382. doi:10.1021/es0704481

Qin, D., and Kang, M. (2017). Application of PhreePlot: Drawing the eh-pH diagram of valence-variable radionuclides. *J. Nucl. Radio.* 39, 113–120.

Rodriguez, D. M., Mayordomo, N., Schild, D., Azzam, S. S. A., Brendler, V., Muller, K., et al. (2021). Reductive immobilization of 99Tc(VII) by FeS2: The effect of marcasite. *Chemosphere* 2021, 130904. doi:10.1016/j.chemosphere.2021.130904

Vanloon, L., Glaus, M., and FerryLatrille, C. (2012). *Studying radionuclides migration on different scales: The complementary roles of laboratory and in site experiments*. doi:10.1533/9780857097194.2.446

Vitorge, P., and Capdevila, H. (2003). Thermodynamic data for modelling actinide speciation in environmental waters. *Radiochim. Acta* 91, 623–632. doi:10.1524/ract.91.11.623.23466

Wang, J., Xu, G. Q., Zheng, H. L., and Fan, X. H. (2005). Geological disposal of high level radioactive waste in China: Progress during 1985-2004. *World. Nucl. Geosci.* 22, 5–16.

Windt, L., Schneider, H., Ferry, C., Catalette, H., Lagneau, V., Poinssot, A., et al. (2006). Modeling spent nuclear fuel alteration and radionuclide migration in disposal conditions. *Radiochim. Acta* 94, 787–794. doi:10.1524/ract.2006.94.9-11.787

Wu, H., Xu, C. Y., Liu, X. H., and Wei, F. X. (2013). Radioactive waste disposal-key to sustainable development of nuclear energy. *Nucl. Saf.* 12, 155–159. doi:10.16432/j.cnki.1672-5360.2013.s1.028

Xie, T., Chen, C., Zhu, J., Shi, Y., Li, T., and Zhang, A. (2021). Adsorption and kinetics of uranium, plutonium and other nuclides on geotechnical media. *J. Nucl. Radio.* 43, 353–361.

Yan, R., Fang, Q., Xie, Y., Wang, S., Li, M., Wu, X., et al. (2022). Approach and mechanism of immobilization of U(VI) by magnetite from aqueous solution. *Uranium. Min. Metall.* doi:10.13426/j.cnki.yky.2022.01.0010

You, W., Peng, W., Tian, Z., and Zheng, M. (2021). Uranium bioremediation with U(VI)-reducing bacteria. *Sci. Total Environ.* 798, 149107. doi:10.1016/j.scitotenv.2021.149107

Yu, T., Yang, J., and Wang, Z. (2020). Adsorption behaviour of Eu(III) on natural bamboo fibres: Effects of pH, humic acid, contact time, and temperature. *Nucl. Sci. Tech.* 31, 4. doi:10.1007/s41365-019-0710-3